Available online at www.sciencedirect.com
SCIENCE DIRECT
Biochemical and Biophysical Research Communications 344 (2006) 283–292
BBRC
www.elsevier.com/locate/ybbrc

Difference in distribution of membrane proteins between low- and high-density secretory granules in parotid acinar cells

Junko Fujita-Yoshigaki [a,*], Osamu Katsumata [a], Miwako Matsuki [b], Tomoyoshi Yoshigaki [a], Shunsuke Furuyama [a], Hiroshi Sugiya [a]

[a] *Department of Physiology, Nihon University School of Dentistry at Matsudo, Matsudo, Chiba 271-8587, Japan*
[b] *Department of Pathology, Tokyo Dental College, Chiba 261-8502, Japan*

Received 24 February 2006
Available online 29 March 2006

Abstract

Secretory granules (SGs) are considered to be generated as immature granules and to mature by condensation of their contents. In this study, SGs of parotid gland were separated into low-, medium-, and high-density granule fractions by Percoll-density gradient centrifugation, since it was proposed that the density corresponds to the degree of maturation. The observation with electron microscopy showed that granules in the three fractions were very similar. The average diameter of high-density granules was a little but significantly larger than that of low-density granules. Although the three fractions contained amylase, suggesting that they are all SGs, distribution of membrane proteins was markedly different. Syntaxin6 and VAMP4 were localized in the low-density granule fraction, while VAMP2 was concentrated in the high-density granule fraction. Immunoprecipitation with anti-syntaxin6 antibody caused coprecipitation of VAMP2 from the medium-density granule fraction without solubilization, but not from Triton X-100-solubilized fraction, while VAMP4 was coprecipitated from both fractions. Therefore, VAMP2 is present on the same granules, but is separated from syntaxin6 and VAMP4, which are expected to be removed from immature granules. These results suggest that the medium-density granules are intermediates from low- to high-density granules, and that the membrane components of SGs dynamically change by budding and fusion during maturation.

Keywords: Parotid acinar cells; Secretory granules; Maturation; Syntaxin6; Vesicle-associated membrane proteins 2 (VAMP2)

In the *trans*-Golgi network (TGN), proteins are sorted and packaged into carrier vesicles for distinct destinations, such as plasma membrane, lysosome, or endosome. In addition to such organelles, the secretory granules (SGs) in cells that have regulated secretion systems such as neuroendocrine, endocrine, and exocrine cells are also the destinations of proteins. SG is a highly specialized storage organelle, from which secretory proteins are released upon stimulation. They have SNARE proteins which may mediate the fusion of granules to target plasma membrane. SGs are not only carriers of secretory proteins, but also machinery for signal-dependent exocytosis. The study of how granules are constructed is important for understanding the regulation of exocytosis.

Electron microscopy (EM) studies showed granules with low electron density in neuroendocrine, endocrine, and exocrine glands [1–4]. γ-Adaptin and procathepsin B, but not mature cathepsin B, are specifically localized at the granules, and vesicles were reportedly seen budding from them in pancreatic β-cells, pancreatic and parotid acinar cells [5]. The organelles that have a low electron density are believed to be immature granules (IMGs) in the process of maturing.

On the other hand, SGs can be separated by density-gradient centrifugation in biochemical studies. In PC12 cells, syntaxin6 and VAMP4 are specifically localized in

* Corresponding author. Fax: +81 47 360 9327.
E-mail address: yoshigaki.junko@nihon-u.ac.jp (J. Fujita-Yoshigaki).

0006-291X/$ - see front matter © 2006 Elsevier Inc. All rights reserved.
doi:10.1016/j.bbrc.2006.03.130

low-density granule fractions [5,6]. It has been reported that pulse-labeled proteins were first detected in low-density fractions and were later detected in high-density fractions in parotid gland [7]. This suggests that newly synthesized proteins are transported from immature (low-density) to mature (high-density) granules, or a granule that includes the pulse-labeled proteins itself changed from an IMG to a mature granule (MG). Therefore, a granule is considered to be generated first as an IMG and then to mature gradually.

The morphology and final size of granules are diverse, depending on the cell type and the contents of the granules. While the size of the MGs in PC12 cells is about 120 nm, and that of granules of insulin in β-cells is 200 nm, salivary parotid or pancreatic acinar cells have much larger secretory granules about 1 μm in diameter. The biogenesis of SG has been well investigated in neuroendocrine cells. In PC12 cells, IMGs bud from the Golgi apparatus as small granules. The diameter of IMGs in neuroendocrine cells is about 80 nm, which is the same as that of coated vesicles [8], suggesting that coat proteins are involved in the budding of IMGs from TGN. The small IMGs fuse with each other in a process called "homotypic" fusion because granules of similar size and character fuse [9]. After the fusion, clathrin-coated vesicles bud from fused IMGs [4,10]. Homotypic fusion is considered to be necessary for the maturation of SG in neuroendocrine cells. In contrast, it is unlikely that IMGs in exocrine acinar cells are generated as coated vesicles. Large, irregularly shaped vacuoles are observed near the Golgi apparatus in EM images [1,2]. IMGs in exocrine cells, such as parotid and pancreatic acinar cells, are considered to first separate from the Golgi apparatus as organelles that have larger sizes than complete granules and to then mature. However, the mechanisms of generation and maturation of SG in exocrine cells have not been understood as well as in neuroendocrine cells, although many EM studies on the exocrine glands have been reported.

SGs in parotid acinar cells have a higher density than in other organelles and are easy to separate biochemically. The contamination of other organelles is very low [11], which is an advantage for the biochemical study of not only the regulatory mechanism of exocytosis, but also for the formation and maturation of granules. In this paper, we separated granules by density-gradient centrifugation according to the method reported by von Zastrow and Castle [7], and examined the distribution of membrane proteins to study the mechanisms of generation and maturation of SG in parotid acinar cells.

Materials and methods

Materials and antibodies. Antibodies to aquaporin5 (AQP5) and *N*-ethylmaleimide-sensitive factor (NSF) were from Chemicon (Temecula, CA) and Stressgen Biotechnologies, respectively. Antibodies against syntaxin6, α-soluble NSF attachment protein (α-SNAP), γ-adaptin, Munc18, GS28, BiP/GRP78, and EEA1 were purchased from BD Biosciences. Anti-Rab3D antibody was purchased from Alexis Biochemicals; antibodies against SNAP-23 and VAMP4 were from Affinity Bioreagents (Deerfield, IL); anti-α-amylase antibody from Sigma. Anti-VAMP2 antibody (anti-SER4253) was prepared as reported previously [12]. Anti-pantophysin antibody was a kind gift from Dr. B. Cheatham (Harvard Medical School), and anti-Rab3A antibody was kindly given by Dr. M. Takahashi (Kitasato University School of Medicine, Japan). Botulinum neurotoxin B (BNT-B) was kindly given by Dr. S. Kozaki (Osaka Prefecture University, Japan).

Separation of SG fractions and preparation of precipitates of SG fractions by centrifugation. The SGs of the rat parotid glands were isolated as described [7], but with a modification. The parotid glands were taken from male Sprague–Dawley rats (200–250 g) anesthetized by sodium pentobarbital (Dainippon Pharmaceutical Co. Ltd, Osaka, Japan). When rats were injected with 0.4 mg isoproterenol (IPR), parotid glands were taken at 8 h after the injection. Homogenization was performed with buffer A (300 mM sucrose, 1 mM $MgCl_2$, 1 mM dithiothreitol (DTT), 1× Complete EDTA-free, and 20 mM MOPS·NaOH, pH 7.0). A part of the postnuclear supernatant was collected, homogenized with low osmotic buffer, added NaCl to 150 mM, and centrifuged at 100,000*g* for 60 min. The pellet was collected as P100 fraction.

The rest of the postnuclear supernatant was centrifuged in 40% Percoll at 16,400*g* for 30 min. The heaviest fraction was collected and recentrifuged in 60% Percoll at 45,500*g* for 30 min. Granule fractions in Percoll-sucrose medium were collected in following three densities: low (1.115–1.125 g/ml), medium (1.125–1.14 g/ml), and high (1.14–1.16 g/ml). Purified granules (Go) were suspended in buffer B (1 mM $MgCl_2$, 1 mM DTT, 1 mM phenylmethanesulfonyl fluoride (PMSF), 1× Complete EDTA-free, and 20 mM Hepes·NaOH, pH 7.4), homogenized, added NaCl to 150 mM, and centrifuged at 100,000*g* for 60 min. The precipitate was used as the granule precipitate fraction (Gp).

Lysosome-rich fraction was prepared as described by Maguire and Luzio [13]. The fraction was homogenized with buffer B, added NaCl to 150 mM, and centrifuged at 100,000*g* for 60 min. The precipitate was suspended in buffer B containing 150 mM NaCl.

Electron microscopy. A pellet of the freshly isolated granules was fixed in modified Karnovsky's fixative solution (2% paraformaldehyde, 2.5% glutaraldehyde in 0.1 M cacodylate buffer, pH 7.4) for 1 h at room temperature. Samples were postfixed in 1% osmium tetraoxide for 60 min, dehydrated with a graded series of ethanol and propylene oxide, and embedded in Epon812. Ultrathin sections were cut with a diamond knife, stained with uranyl acetate and lead citrate, and then examined with a transmission electron microscope (JEOL JEM-1010).

Particle size analysis by photon correlation spectroscopy. The sizes of SGs were measured by the photon correlation spectroscopy instrument N5 (Beckman Coulter, USA). SGs were suspended in 1 ml of buffer A and transferred to a plastic cuvette at room temperature. The cuvette was set in N5 and a 25 mV Helium–Neon laser beam was directed at it, and scattering light at an angle of 90° was analyzed.

Immunofluorescence microscopy. Granules were attached to coverslips by Cell-TAK. After fixation with 10% formalin/PBS, granules were permeabilized with 0.2% Triton X-100/PBS, blocked with 1% BSA-0.05% goat IgG, and labeled with anti-amylase antibody (1:50) followed by Alexa Fluor® 488-anti-rabbit IgG. Fluorescence images were acquired by μRadiance MR/AG-2/S confocal microscopy (Bio-Rad).

Immunoprecipitation from solubilized Gp fractions. Gp fractions were suspended in solubilizing buffer C (150 mM NaCl, 1 mM EDTA, 1 mM EGTA, 1 mM DTT, 1 mM PMSF, and 20 mM Hepes·NaOH, pH 7.4) containing 4% Triton X-100 and incubated for 45 min. Unsolubilized materials were removed by centrifugation (20,000*g* for 15 min). The supernatants were dialyzed against buffer C containing 1% Triton X-100 overnight. After centrifugation at 20,000*g* for 15 min, the supernatants were obtained as solubilized Gp fractions. Solubilized Gp fractions (20 μg) were suspended in reaction buffer (150 mM NaCl, 20 mM NaF, 10 mM $MgCl_2$, 2 mM ATP, 1 mM PMSF, 1 mM DTT, 1 mM EGTA, 1% Triton X-100, and 20 mM Hepes·NaOH, pH 7.4). Samples were added to protein A-Sepharose 4FF conjugated with normal mouse or rabbit IgG and were incubated at 4 °C for 60 min. After centrifugation, the supernatants were recovered and incubated with anti-syntaxin6 antibody conjugated with

protein A-Sepharose 4FF at 4 °C for 2 h. Following this, protein A-Sepharose was collected by centrifugation and boiled in sample buffer for SDS–PAGE.

For immunoprecipitation from non-solubilized granule fractions, Protein A Magnet Beads (New England Biolabs) were used. All procedures were performed in Buffer A.

Immunoblotting. For the immunoblotting of pantophysin, samples in SDS–PAGE sample buffer were diluted and incubated overnight at 37 °C in glycosidase buffer (1% Triton X-100, 1 mM PMSF, and 20 mM Hepes·NaOH, pH 7.2) containing 2 U of *N*-glycosidase F (Roche), because rat pantophysin has N-linked glycosylation and variable processing [14]. Reactions were stopped by the addition of SDS–PAGE sample buffer.

The proteins were separated on SDS–PAGE, transferred to Hybond-P (Amersham), and blotted with antibodies. Immunoreactivity was determined by means of the ECL or ECL Plus chemiluminescence reactions (Amersham). For quantitative analysis, ECF Western blotting kit (Amersham) was used and the intensity of fluorescence was determined by Image Analyzer 595S (Molecular Dynamics).

Calculation of the proportions of granule membrane proteins that were present in the Gp fractions. The percentage of VAMP2, VAMP4, and syntaxin6 present in Gp of SG fractions to the total precipitate fraction (P100), which was taken as 100%, was calculated from the total protein (mg) and specific activity of each protein in the three fractions (Tables 1 and 2).

Table 1
Total amounts of protein in P100 and Gp fractions of LDG, MDG, and HDG fractions

Fraction	Total protein[a] (mg)	Relative value[b]
P100	37.5 ± 1.0	1
LDG	0.022 ± 0.003	5.87×10^{-4}
MDG	0.071 ± 0.012	1.89×10^{-3}
HDG	0.162 ± 0.022	4.32×10^{-3}

[a] The amounts of total proteins recovered from eight rats. The values were shown as averages of eight independent experiments.
[b] The values were shown as relative values to the amounts of total proteins in P100 which was taken as 1.

Table 2
Presence of marker proteins or enzymes of organelles in Gp of the three granule fractions

	LDG	MDG	HDG
Marker proteins[a]			
Na^+-K^+-ATPase β1	n.d.	n.d.	n.d.
BiP/GRP78	0.081 ± 0.013	0.062 ± 0.013	0.026 ± 0.014
GS28	n.d.	n.d.	n.d.
EEA1	n.d.	n.d.	n.d.
Marker enzymes[b]			
N-Acetyl-β-glucosaminidase	1.41 ± 0.21	0.91 ± 0.16	0.44 ± 0.10
Succinate dehydrogenase	n.d.	n.d.	n.d.
Granule proteins[a]			
VAMP2	28.2 ± 7.0	78.7 ± 23.4	155.8 ± 25.1
VAMP4	59.9 ± 10.5	46.1 ± 13.5	7.1 ± 2.2
Syntaxin6	15.3 ± 1.0	6.3 ± 1.8	1.2 ± 0.63
Amylase	3.07 ± 0.12	3.27 ± 0.07	3.33 ± 0.12

n.d., not detected.
[a] Immunoreactivities in Gp of each granule fraction are shown as relative values to that in P100 which was taken as 1 when the same amounts of proteins in each fraction were used.
[b] Enzyme activities were measured as described in Materials and methods, and the specific activities per milligram protein detected in Gp of each granule fraction are shown as relative values to that in P100 which was taken as 1.

VAMP2:

$$(28.2 * 5.87 \times 10^{-4} + 78.7 * 1.89 \times 10^{-3} + 155.8 * 4.32 \times 10^{-3})/1 * 1 = 0.836,$$

VAMP4:

$$(59.9 * 5.87 \times 10^{-4} + 46.1 * 1.89 \times 10^{-3} + 7.1 * 4.32 \times 10^{-3})/1 * 1 = 0.153,$$

syntaxin6:

$$(15.3 * 5.87 \times 10^{-4} + 6.3 * 1.89 \times 10^{-3} + 1.2 * 4.32 \times 10^{-3})/1 * 1 = 0.026.$$

The percentage of VAMP2, VAMP4, and syntaxin6 present in the three granule fractions was estimated 83.6%, 15.3%, and 2.6%.

Statistics. Statistical testing was performed using the Bonferroni method after a factorial analysis of variance (ANOVA). Numbers given in the text represent means ± SEM.

Results

Separation of granules by Percoll-density gradient centrifugation

To study how SGs are generated, they were separated by density-gradient centrifugation into three: low-density granule (LDG), medium-density granule (MDG), and high-density granule (HDG) fractions. The purity was confirmed by electron-microscopic observation (Figs. 1A–C). All three granule fractions were almost devoid of other organelles. The morphology of the three fractions was similar and there was no apparent difference. The diameters of the granule sections were measured and the mean values calculated. Although the diameter estimated from the sections must be smaller than the actual diameter of the granules, they must correlate with each other. The mean value of the HDG diameters (800 ± 8 nm, $n = 500$) was significantly greater than those of MDG (745 ± 9 nm, $n = 485$) and LDG (739 ± 9 nm, $n = 444$) ($p < 0.0001$), although granules whose diameters were larger than 1 μm were occasionally observed in all fractions (Fig. 1D). Because it is likely that the size of SG was changed by fixation, the diameters were measured by another method without fixation. Submicron Particle Size Analyzer N5 (Beckman–Coulter) is an instrument for determining the size of particles by measuring their diffusion constants in solution. The mean sizes of the particles in LDG, MDG, and HDG fractions were calculated (Fig. 1E). The average diameter of HDG was significantly greater than that of MDG and LDG ($p < 0.0001$).

Presence of amylase in all three granule fractions

To confirm that the purified fractions were SGs, the presence of amylase in the granules was examined by immunofluorescence microscopy. Granules of all three fractions were stained by anti-amylase antibody (Fig. 2). The DIC images of granules corresponded to the amylase staining, indicating that the granules of the three fractions were secretory granules. The total amylase activities of

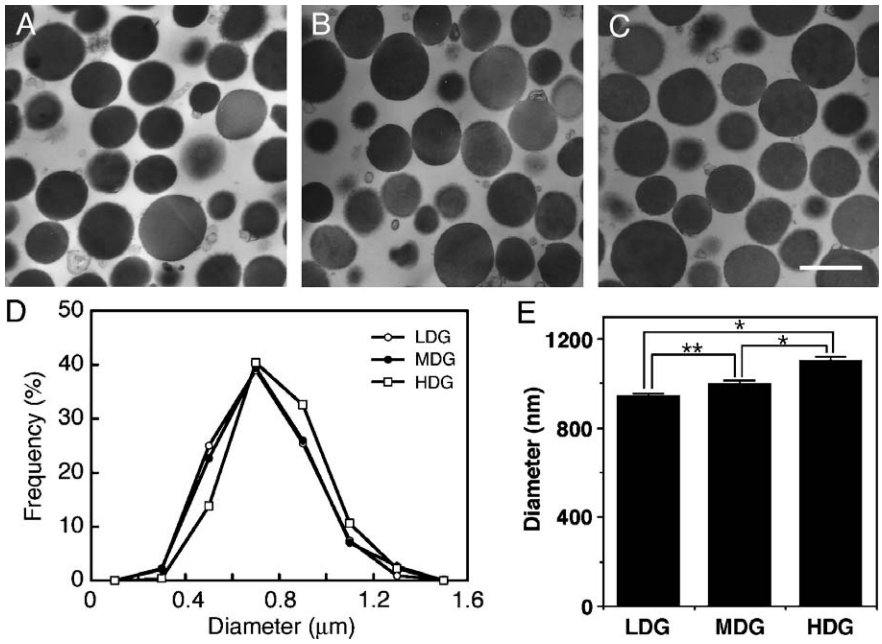

Fig. 1. LDG, MDG, and HDG separated by Percoll-density gradient centrifugation were morphologically similar except for their diameters. (A–C) Electron microscopy images of the LDG (A), MDG (B), and HDG (C) fractions. Bar, 1 μm. (D) Diameters measured from the ultrathin sections of LDG (open circles), MDG (closed circles), and HDG (open squares). Data were obtained from 10 or 11 sections derived from eight rats. The values were normalized to the total number of granules. (E) The mean sizes of particles in LDG, MDG, and HDG fractions were measured by submicron particle size analyzer N5. The indicated values are the averages of data from three independent preparations. The higher the density was, the larger the diameter was (*$p < 0.0001$, **$p < 0.001$).

MDG and LDG were one-fourth and one-thirteenth of that of HDG, respectively (Fig. 3A). The distribution of amylase activity represents the population of the three fractions of granules. The specific activities of amylase in LDG, MDG, and HDG fractions were 250 ± 6.1, 251 ± 5.3, and 254 ± 9.1 U/mg protein, respectively (Fig. 3B). No significant differences were seen among them. The yield of purification was about 3.3–3.4 times, since the specific activity of homogenate of the parotid gland was 75.1 ± 8.0 U/mg protein. The total proteins in the three fractions were compared by SDS–PAGE and Coomassie brilliant blue staining. The patterns were similar among the three fractions (data not shown). Only a band whose apparent molecular weight was 22 kDa was a little more concentrated in LDG fractions as reported previously [7].

After the lysis of granules by homogenization in a low osmotic solution, the precipitate (Gp) fractions of centrifugation at 100,000*g* were collected, which are expected to include membrane proteins. The proportion of the amount of proteins in the precipitate fraction to that in the whole granule fraction (Gp/Go) was calculated. The value of Gp/Go of LDG was the highest among that of the three fractions (Fig. 3C). A part of secretory proteins was precipitated by the centrifugation because amylase was also detected in the Gp fractions. The amounts of amylase per milligram proteins in Gp of the three granule fractions were examined by immunoblotting analysis (Table 2). There was no significant difference in the amount of amylase among the three fractions, suggesting that the amounts of contamination of secretory proteins in the Gp fractions are similar. Therefore, the difference in Gp/Go among the three fractions possibly implies not the degree of contamination of secretory proteins, but degree of condensation of the contents, size of the granules, or concentration of membrane proteins.

Distribution of membrane proteins in the three granule fractions

To investigate the difference of the three granule fractions, the presence of membrane proteins in the Gp fractions was examined by immunoblotting. As a result, the distribution of membrane proteins differed markedly among the three fractions. The concentrations of VAMP2, SNAP-23, Munc18, Rab3A, and Rab3D were higher in the HDG fraction (Fig. 4A). These proteins may be involved in the fusion of granules and plasma membrane. The concentration of such proteins during maturation is to be expected. AQP5 and pantophysin are also detected much more in HDG. In contrast, syntaxin6, γ-adaptin are, as previously reported [5], not present in the HDG fraction (Fig. 4A). By immunoblotting with anti-VAMP4 antibody, two bands were detected. Since the lower band had the same apparent molecular weight as VAMP2 in electrophoresis, it was expected to be VAMP2. The upper band, which probably corresponds to VAMP4, was concentrated in the LDG fraction. The differences in the amounts of

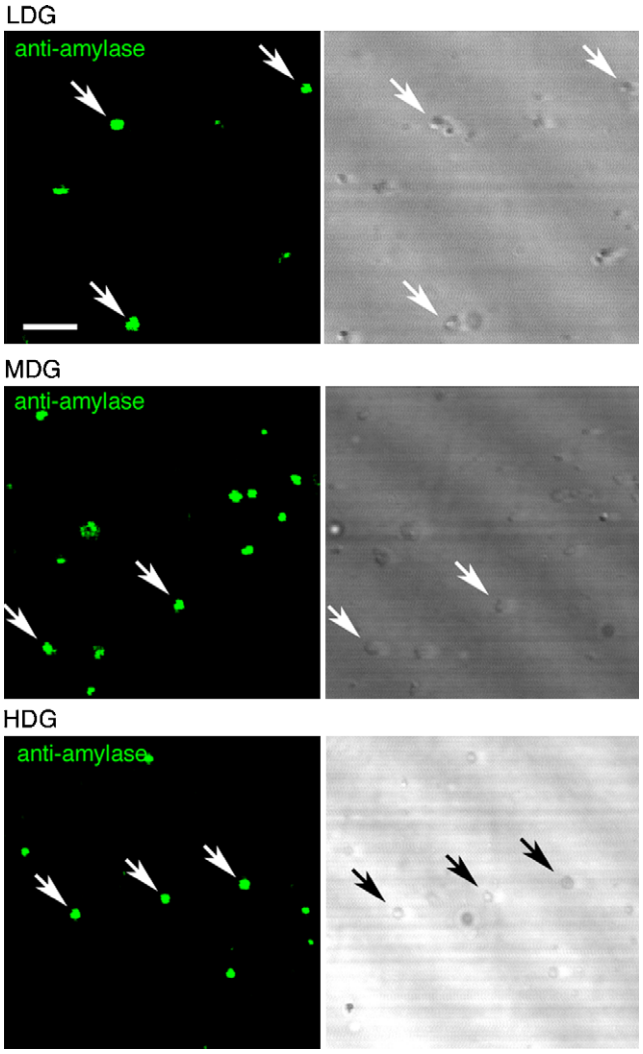

Fig. 2. The granules in all three fractions contained amylase. DIC images and immunofluorescence microscopy of low- (top panels), medium- (middle panels), and high- (bottom panels) density granule fractions. Granules in all the three fractions were stained with anti-amylase antibody. Bar, 5 μm.

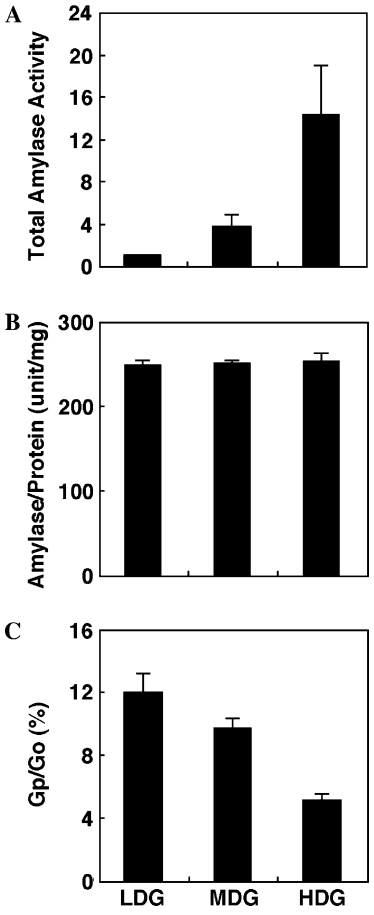

Fig. 3. Amylase activities and protein concentrations in the three granule fractions. (A) Total amylase activities in the three fractions are shown as values relative to that of LDG. (B) Relative amylase activities per milligram of protein. (C) Relative amounts of proteins in precipitate fractions (Gp) to that of the total proteins of the granule fractions (Go). Values were averages of data obtained from 10 independent experiments.

α-SNAP and NSF among three fractions are smaller than those with other proteins, but the amounts in LDG fraction are a little larger.

Fig. 4B shows the comparison of the amounts of VAMP2 and syntaxin6 in the three fractions. The amounts of VAMP2 and syntaxin6 were represented as a percentage to that in HDG and LDG, respectively, which were taken as 100. The amount of VAMP2 increases according to the density, in proportion to reduction of syntaxin6. This result suggests that the granules in LDG and HDG fractions are completely different although they have very similar amylase activity. The MDG seems an intermediate or a mixture of LDG and HDG.

To confirm that the difference of membrane proteins is not due to the contamination of other organelles, the presence of marker proteins of other organelles was examined. Na^+-K^+-ATPase β1, a marker enzyme of plasma membrane, was not detected by immunoblotting analysis (Table 2). The enzyme activity of K^+-dependent phosphatase, another plasma membrane marker, was neither detected in the granule fractions (data not shown). Neither Golgi marker p115 (data not shown), GS28, nor early endosome (EE) marker EEA1 was detected (Table 2). The enzyme activity of succinate dehydrogenase, a marker enzyme of mitochondria, was not detected. BiP/GRP78, a marker protein of ER, were detected in the Gp fractions (Table 2), but the amount of BiP/GRP78 per milligram protein in the Gp fraction of LDG is only one-twelfth of the P100 fraction. It is expected that the contamination of other intracellular organelles than SGs was very low. Syntaxin6 is reported to be localized at TGN or EE [15,16]. Because no marker proteins of either type of organelle were detected in the LDG fraction, the detection of syntaxin6 could not have been the result of contamination of such organelles.

Only the specific activity of *N*-acetyl-β-glucosaminidase, a marker enzyme of lysosome, is higher in the Gp of LDG than that in the P100 fraction (Table 2), which indicates that lysosomes are present in LDG. The contamination may be due to similarity of the density of lysosome and

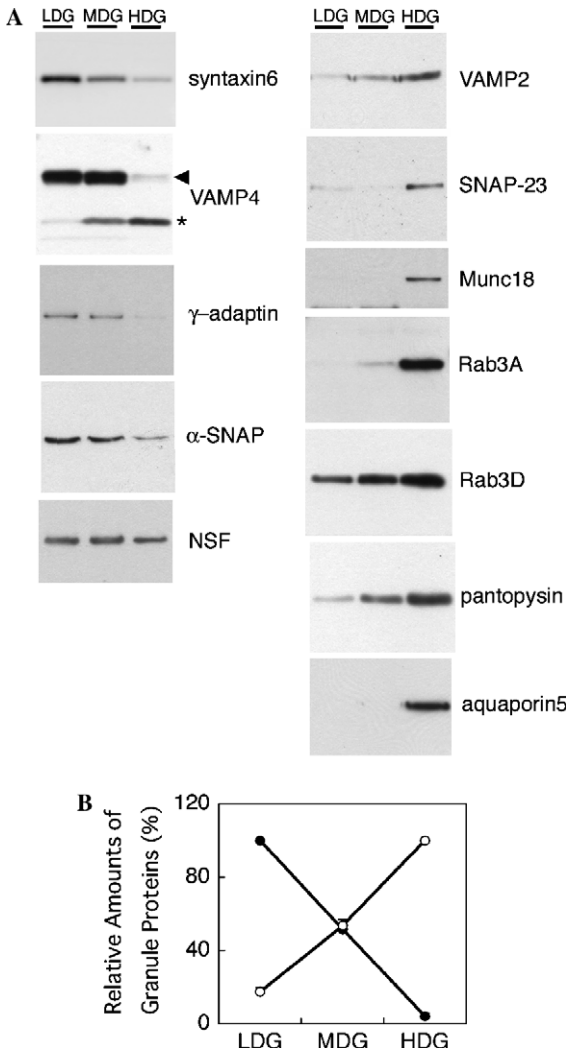

Fig. 4. Distribution of membrane proteins among the three SG fractions. (A) For Gp fractions of LDG, MDG, and HDG, the same amounts (0.1– 4 μg proteins) were electrophoresed in each lane. The antibody against VAMP4 detected two bands. The electrophoretic mobility of the lower band (asterisk) was identical with that of the band detected by anti-VAMP2 antibody. The upper band (arrowhead) is suggested to be VAMP4. (B) Relative amounts of VAMP2 (open circles) and syntaxin6 (closed circles) to that present in the Gp fractions of HDG and LDG that were taken as 100%, respectively. Values were means of data from three independent experiments.

LDG. However, lysosome-rich fraction that was partially purified by another method [13] had more than 10 times higher activity of *N*-acetyl-β-glucosaminidase (16.2 ± 0.4 compared with the activity in P100 which was taken as 1) than that of Gp of LDG. Therefore, the presence of lysosomes in Gp of LDG is less than 10% at the most. Immunoblotting analysis showed that the presence of syntaxin6 and VAMP4 in lysosome-rich fraction was only 0.62 ± 0.44 and 2.0 ± 0.1 compared with the activity in P100 which was taken as 1, i.e., their amounts were less than one-tenth of that in Gp of LDG. This result indicates that the higher concentration of the two proteins in LDG than HDG is not due to the contamination of lysosomes. Furthermore, the lower concentration of VAMP2 in LDG is not either due to the contamination of other organelles such as lysosome and ER because the degree of contamination of the two organelles is lower compared with the difference in the amount of VAMP2 between LDG and HDG.

The recovery of VAMP2, VAMP4, and syntaxin6 present in the three granule fractions was estimated 83.6%, 15.3%, and 2.6% to the total protein in P100 fraction, which may correspond to total membranes except for nuclear, as described in Materials and methods. This result shows that most of VAMP2 is localized at SGs whereas only a part of VAMP4 and syntaxin6 are localized at SGs. Syntaxin6 and VAMP4 are reported to be localized at TGN and be involved in transport between TGN and EE [15–17]. Therefore, the low percentage of recovery of VAMP4 and syntaxin6 in the granule fractions is consistent with the previous reports.

Interaction of VAMP4 and syntaxin6 on the secretory granules

VAMP4 and syntaxin6 are colocalized at LDG fractions, as Fig. 4 shows. Syntaxin6 was reported to interact with many kinds of SNARE proteins, one of which is VAMP4 [6]. Therefore, we wished to ascertain whether syntaxin6 and VAMP4 interact at granule membranes. Immunoprecipitation with anti-syntaxin6 antibody from the three granule fractions, which were solubilized with Triton X-100, was performed. Syntaxin6 was efficiently precipitated from the solubilized LDG fraction (Fig. 5A). Syntaxin6 was hardly detected in the immunoprecipitates from the HDG fraction. VAMP4 was coprecipitated with anti-syntaxin6 antibody, and the amounts of coprecipitated VAMP4 were large in LDG and small in HDG in proportion to that of precipitated syntaxin6. The lower band, detected with anti-VAMP4 antibody, which is expected to be VAMP2, was less effectively coprecipitated than VAMP4. Using anti-VAMP2 antibody, VAMP2 was detected in the immunoprecipitates. Although there is less VAMP2 in LDG than in HDG, more VAMP2 was coprecipitated from LDG than from HDG with anti-syntaxin6 antibody. VAMP2's efficiency of coimmunoprecipitation seems to be lower than that of VAMP4, because the amount of the precipitated VAMP2 was small compared to its amounts present in the starting Gp fractions used for the immunoprecipitation.

To determine whether the lower band detected with the antibody to VAMP4 is really VAMP2, a cleavage assay with BNT-B was performed. BNT-B is known to cleave specifically between Gln76 and Phe77 of VAMP2. Although the homology between VAMP2 and VAMP4 is very high, VAMP4 does not have the cleavage site where BNT-B can act. On incubation of the Gp fraction of HDG with activated BNT-B, the intensity of the band detected with anti-VAMP2 antibody decreased (Fig. 5B, left). The lower band detected with anti-VAMP4

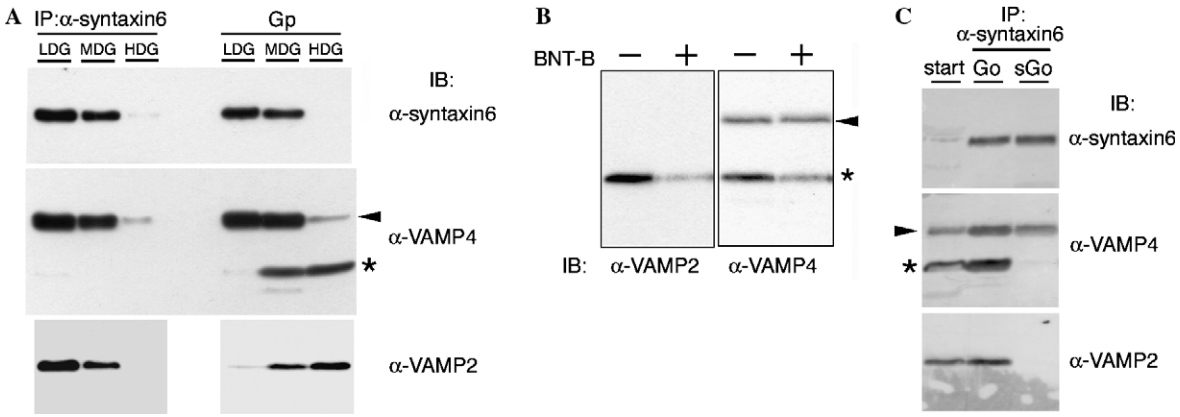

Fig. 5. Binding of syntaxin6 and VAMP4 on the secretory granule membrane. (A) Coimmunoprecipitation of VAMP4 and VAMP2 from solubilized Gp fractions of LDG, MDG, and HDG (7.5 μg each) with the antibody against syntaxin6. To see the efficiency of coprecipitation, starting Gp samples (2 μg each for immunoblotting with anti-syntaxin6 or VAMP4 antibodies, 0.4 μg each for that with anti-VAMP2 antibody) were applied for immunoblotting (IB) as well as precipitated samples (IP). (B) Cleavage analysis using BNT-B. Gp fractions of HDG were incubated with inactivated (−) and activated (+) BNT-B and applied for immunoblotting with anti-VAMP2 (left) or VAMP4 (right) antibody. (C) Coprecipitation of VAMP2 with syntaxin6 from non-solubilized (Go), but not from solubilized (sGo) Go fractions. Precipitates from the Go (30 μg) and sGo (60 μg) fractions of MDG were separated by electrophoresis, transferred, and blotted with antibodies against syntaxin6, VAMP4, and VAMP2. To see the efficiency of precipitation, the starting Go sample (8 μg each for immunoblotting with anti-syntaxin6 or VAMP4 antibodies, 4 μg for anti-VAMP2 antibody) was applied. The upper bands (asterisk) and lower bands (arrowhead) detected by ant-VAMP4 antibody are expected to correspoond to VAMP4 and VAMP2, respectively.

antibody was specifically diminished whereas the upper band did not change (Fig. 5B, right). Thus, it was seen that the lower band corresponded to VAMP2. Since the efficiency of coimmunoprecipitation of VAMP4 is higher than that of VAMP2, it is suggested that VAMP4 has higher affinity for syntaxin6 than VAMP2 has on the membrane of SGs.

To examine whether VAMP2 and syntaxin6 are localized on the same SG in the MDG fraction, syntaxin6-positive granules were prepared from non-solubilized granule fractions (Go). Pellet of MDG was divided to two fractions, one of which was then solubilized by 1% Triton X-100 (sGo), and immunoprecipitation with anti-syntaxin6 antibody from the Go and sGo fractions was performed. The amounts of syntaxin6, VAMP4, and VAMP2 in the precipitates were examined by immunoblotting analysis. Syntaxin6 and VAMP4 were precipitated from both of Go and sGo fractions (Fig. 5C). VAMP2 was scarcely precipitated from sGo as well as from solubilized Gp fractions (Figs. 5A and C). However, VAMP2 was detected in the immunoprecipitates from the Go fraction. The ratio of VAMP4 and VAMP2 in the precipitates from Go was similar to that in the starting Go fraction. This result indicates that VAMP2 is present on the syntaxin6-positive granules in MDG, while VAMP2 does not interact with syntaxin6 on SG. It is likely that MDG is not the mixture, but the intermediate of LDG and HDG.

Three granule fractions isolated from the rats injected with isoproterenol (IPR)

The size of secretory granules is variable and depends on physiological conditions. For example, starvation and chronic stimulation with IPR, one of the β-adrenergic agonists, increased the size of granules [18]. Moreover, granules in both pancreas and parotid acinar cells in Rab3D-knockout mice are larger than those of wild-type mice [19]. On the contrary, injection of 0.4 mg IPR to rats in vivo caused depletion of SGs following new formation of granules, which are obviously smaller than 1 μm at 8 h after the injection (data not shown). To examine the relationship between density and size of SGs, SGs were isolated from the rats at 8 h after the injection, and were separated to low-density (1.115–1.125 g/ml), medium-density (1.125–1.14 g/ml), and high-density (1.14–1.16 g/ml) granule fractions (iLDG, iMDG, and iHDG, respectively) in the exactly same manner as the control condition. SGs in the three fractions were observed by EM. Although all the three fractions contained smaller SGs, the difference in their diameters among the fractions was clearer than in the control (Figs. 6A–C). Fig. 6D shows the distribution of diameter of granules in the three fractions. The average diameters of iLDG (533 ± 7 nm, $n = 745$) and iMDG (577 ± 7 nm, $n = 790$) were significantly smaller than that of iHDG (670 ± 7 nm, $n = 856$) ($p < 0.0001$). Granules that have lower density are smaller than in high-density fractions in IPR-injected rats as well as those in the control rats.

To examine the distribution of membrane proteins, precipitate fractions were prepared by centrifugation at 100,000*g*. Immunoblotting analysis by anti-syntaxin6 and anti-VAMP2 antibodies showed similar results to the control (Fig. 6E). The amount of syntaxin6 was larger in iLDG, and VAMP2 was concentrated in the iHDG fraction. Therefore, the distribution of membrane proteins was similar to the control although the size of SGs in all the three fractions was smaller than LDG under the control condition.

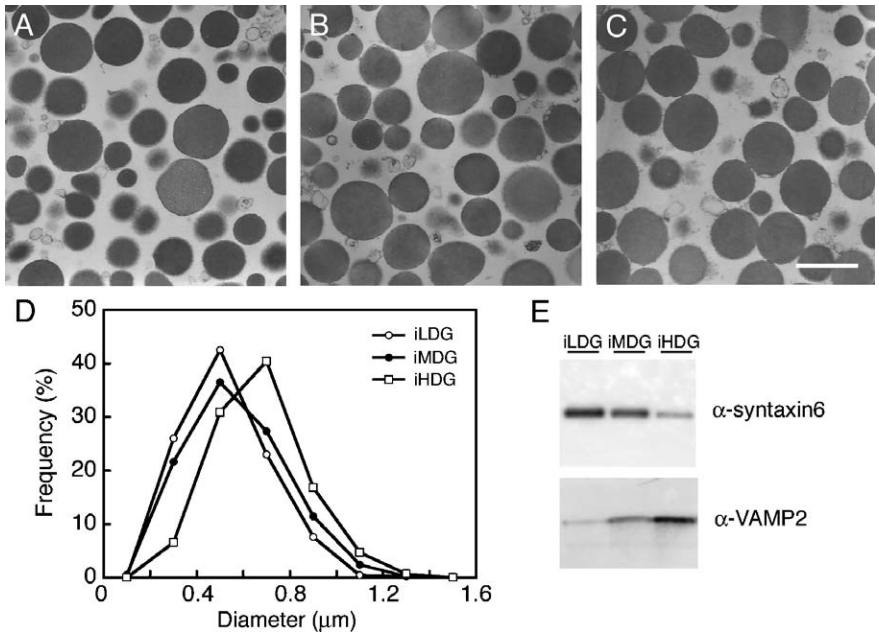

Fig. 6. iLDG, iMDG, and iHDG isolated from the rats injected with IPR. (A–C) Electron microscopy images of iLDG (A), iMDG (B), and iHDG (C) fractions. Bar, 1 μm. (D) Distribution of diameters measured from the ultrathin section of iLDG (open circles), iMDG (closed circles), and iHDG (open squares). The values were normalized to the total number of granules. (E) Distribution of syntaxin6 and VAMP2 among the three fractions. The same amounts of proteins were electrophoresed in each lane.

Discussion

In the present study, SGs were separated to three fractions by Percoll-density gradient centrifugation. The distribution of membrane proteins among the three fractions was markedly different (Fig. 4). Because the contamination of other organelles was low, the difference in membrane proteins probably depends on the difference in granules themselves. The distribution of VAMP2 and syntaxin6 suggests that LDG and HDG are completely different although both of them contain amylase and their morphology is very similar. SGs from the IPR-stimulated rats were also isolated and separated to three fractions. Although the diameters in all the three fractions were smaller, the pattern of distribution of membrane proteins was the same to that of the control SGs (Fig. 6). These results suggest that the distribution of membrane proteins depends on the density of SGs, but not on their size.

From following two reasons, LDG is expected to be IMG. First, von Zastrow and Castle [7] showed that newly synthesized proteins move from LDGs to HDGs time-dependently. Second, injection of IPR into rats in vivo causes obsolescence of the parotid glands and depletion of granules. Several hours after the injection, granules were recovered and the proportion of lower-density granules was higher than before the injection.[1] It is, therefore, likely that an LDG is an IMG that will become an MG.

In general, however, IMG in exocrine cells is considered to be larger than MG from the previous studies. The in situ images of electron microscopy showed that IMGs, which are irregularly shaped and whose electron density is low, are larger than MGs. SGs in exocrine glands are considered to be derived from the TGN as large, irregularly shaped vacuolar structures [2]. The vacuoles are considered to mature by condensing the intravesicular protein concentration with a reduction of size. In our study, however, the diameter of LDG was smaller than that of HDG (Figs. 1D and E). The contradiction about granule size suggests that the IMGs showed in EM are not necessarily identical with LDG separated biochemically. There is a possibility that the most LDGs isolated by centrifugation are assigned as MGs in EM images because the morphology of LDG and HDG is very similar.

Nevertheless, the components of membrane proteins differ completely among the three fractions. Supposing that LDG is IMG, dynamic exchange of membrane components occurs after the generation of IMGs, although LDGs seem static. Arf1, which is not usually detected in granule membrane fractions, is translocated from the cytosol to the granule membrane in the presence of GTPγS [11]. Arf1 may be involved in the formation of coated vesicles that bring out unnecessary proteins from SGs. It was reported that AP-1 was found on the clathrin-coated membrane buds emerging from IMGs [5], and constitutive-like vesicles were separated from IMGs and transported to plasma membranes [7,20]. Translocation of the proteins from IMGs to each of the destinations such as EEs, lysosomes, and plasma membranes suggests that the membrane

[1] O. Katsumata, J. Fujita-Yoshigaki, M. Hara-Yokoyama, M. Yanagishita, S. Furuyama, H. Sugiya, in preparation.

of SG is the site for sorting proteins [21]. At the same time, if LDG becomes HDG, membrane lipids should be supplied somehow because HDGs are a little larger than LDGs. Homotypic fusion of SGs or fusion of small vesicles to IMG may be necessary for maturation. Maturation is possibly not only the removal of proteins that are delivered passively, but also the concentration of contents and membrane proteins that may function in fusion to plasma membrane. For example, VAMP2, which was shown to be essential for cAMP-dependent amylase secretion [22], accumulated in HDG. There is a possibility that the vesicles that supply such components probably fuse with IMGs after generation of IMGs.

Although the MDG fraction contains both of VAMP2 and VAMP4, syntaxin6 binds to VAMP4 more efficiently than to VAMP2 (Fig. 5A). The affinity of VAMP2 to syntaxin6 seems to be lower than that of VAMP4. Otherwise, this result suggests that syntaxin6 does not encounter VAMP2 on SGs. If so, there are two possible explanations for that. One possibility is that syntaxin6 and VAMP2 are localized on different SGs in MDG. However, immunoprecipitation from non-solubilized granule fraction with anti-syntaxin6 antibody caused coprecipitation of VAMP2 (Fig. 5C), suggesting that VAMP2 is present on the same SGs as syntaxin6. Another possibility is that syntaxin6 and VAMP4 are separated from VAMP2 on the same SGs. Membrane microdomains, also called rafts, are considered to separate specific membrane proteins from others on the membrane surface for various cell functions including membrane traffics [23,24]. If MDG is an intermediate from LDG to HDG, syntaxin6 and VAMP4 will be removed from MDG. It is likely that such proteins to be removed are separated by membrane microdomains from other proteins to be retained.

What is the meaning of the presence of syntaxin6 and VAMP4 on IMG? It is not likely that the presence of such proteins is only a result of missorting at the formation of IMG from TGN. Syntaxin6 was reported to mediate homotypic fusion of IMG in PC12 cells [25]. The possibility that syntaxin6 is necessary for new secretory granules in pancreatic β-cell was also proposed [26]. There is a possibility that syntaxin6 is essential for generation or maturation of SG.

As well as SGs from the control rats, iLDG isolated from IPR-injected rats was smaller than iHDG. It is unlikely that iHDG is MG, since its size is smaller than that of the normal SGs. However, its density and distribution of membrane proteins are consistent with the control HDG (Fig. 6E). Therefore, size and density of SGs are determined independently. It is also unlikely that the larger SGs from chronically stimulated rats or Rab3D-deficient mice are normal MGs. It is interesting to separate the unusual SGs to LDG, MDG, and HDG fractions and to investigate membrane protein distribution. Such an analysis will give useful information on the regulatory mechanism to control the size and density of SGs.

Acknowledgments

This work was supported by Grants-in-Aid for scientific research from the Ministry of Education, Science, Culture, Sports and Technology of Japan (16591868, 16791135); by a Suzuki Memorial Grant of Nihon University School of Dentistry at Matsudo (Joint Research Grant for 2003); and by a Grant-in-Aid for a 2001 Multidisciplinary Research Project from MEXT.

References

[1] G.C. Lucien, G.E. Palade, Protein synthesis, storage, and discharge in pancreatic exocrine cell: an autoradiographic study, J. Cell Biol. 20 (1964) 473–495.
[2] G. Palade, Intracellular aspects of the process of protein synthesis, Science 189 (1975) 347–358.
[3] P. Arvan, J.D. Castle, Protein sorting and secretion granule formation in regulated secretory cells, Trends Cell Biol. 2 (1992) 327–331.
[4] S.A. Tooze, G.J. Martens, W.B. Huttner, Secretory granule biogenesis: rafting to the SNARE, Trends Cell Biol. 11 (2001) 116–122.
[5] J. Klumperman, R. Kuliawat, J.M. Griffith, H.J. Geuze, P. Arvan, Mannose 6-phosphate receptors are sorted from immature secretory granules via adaptor protein AP-1, clathrin, and syntaxin 6-positive vesicles, J. Cell Biol. 141 (1998) 359–371.
[6] F. Wendler, S.A. Tooze, Syntaxin 6: the promiscuous behaviour of a SNARE protein, Traffic 2 (2001) 606–611.
[7] M. von Zastrow, J.D. Castle, Protein sorting among two distinct export pathways occurs from the content of maturing exocrine storage granules, J. Cell Biol. 105 (1987) 2675–2684.
[8] S.A. Tooze, T. Flatmark, J. Tooze, W.B. Huttner, Characterization of the immature secretory granule, an intermediate in granule biogenesis, J. Cell Biol. 115 (1991) 1491–1503.
[9] S. Urbe, L.J. Page, S.A. Tooze, Homotypic fusion of immature secretory granules during maturation in a cell-free assay, J. Cell Biol. 143 (1998) 1831–1844.
[10] A.S. Dittie, N. Hajibagheri, S.A. Tooze, The AP-1 adaptor complex binds to immature secretory granules from PC12 cells, and is regulated by ADP-ribosylation factor, J. Cell Biol. 132 (1996) 523–536.
[11] Y. Dohke, M. Hara-Yokoyama, J. Fujita-Yoshigaki, R.A. Kahn, Y. Kanaho, S. Hashimoto, H. Sugiya, S. Furuyama, Translocation of Arf1 to the secretory granules in rat parotid acinar cells, Arch. Biochem. Biophys. 357 (1998) 147–154.
[12] J. Fujita-Yoshigaki, Y. Dohke, M. Hara-Yokoyama, S. Furuyama, H. Sugiya, Presence of a complex containing vesicle-associated membrane protein 2 in rat parotid acinar cells and its disassembly upon activation of cAMP-dependent protein kinase, J. Biol. Chem. 274 (1999) 23642–23646.
[13] G.A. Maguire, J.P. Luzio, The presence and orientation of ecto-5'-nucleotidase in rat liver lysosomes, FEBS Lett. 180 (1985) 122–126.
[14] C.C. Brooks, P.E. Scherer, K. Cleveland, J.L. Whittemore, H.F. Lodish, B. Cheatham, Pantophysin is a phosphoprotein component of adipocyte transport vesicles and associates with GLUT4-containing vesicles, J. Biol. Chem. 275 (2000) 2029–2036.
[15] A. Simonsen, J.M. Gaullier, A. D'Arrigo, H. Stenmark, The Rab5 effector EEA1 interacts directly with syntaxin-6, J. Biol. Chem. 274 (1999) 28857–28860.
[16] F. Mallard, B.L. Tang, T. Galli, D. Tenza, A. Saint-Pol, X. Yue, C. Antony, W. Hong, B. Goud, L. Johannes, Early/recycling endosomes-to-TGN transport involves two SNARE complexes and a Rab6 isoform, J. Cell Biol. 156 (2002) 653–664.
[17] J.B. Bock, J. Klumperman, S. Davanger, R.H. Scheller, Syntaxin 6 functions in *trans*-Golgi network vesicle trafficking, Mol. Biol. Cell 8 (1997) 1261–1271.

[18] G.D. Bloom, B. Carlsoo, A. Danielsson, H. Gustafsson, R. Henriksson, Quantitative structural analysis and the secretory behaviour of the rat parotid gland after long and short term isoprenaline treatment, Med. Biol. (Helsinki) 57 (1979) 224–233.
[19] D. Riedel, W. Antonin, R. Fernadez-Chacon, G. Alvarez de Toledo, T. Jo, M. Geppert, J.A. Valentijn, K. Valentijn, J.D. Jamiesen, T.C. Südhof, R. Jahn, Rab3D is not required for exocrine exocytosis but for maintenance of normally sized secretory granules, Mol. Cell. Biol. 22 (2002) 6487–6497.
[20] A.Y. Huang, A.M. Castle, B.T. Hinton, J.D. Castle, Resting (basal) secretion of proteins is provided by the minor regulated and constitutive-like pathways and not granule exocytosis in parotid acinar cells, J. Biol. Chem. 276 (2001) 22296–22306.
[21] R. Kuliawat, J. Klumperman, T. Ludwig, P. Arvan, Differential sorting of lysosomal enzymes out of the regulated secretory pathway in pancreatic β-cells, J. Cell Biol. 137 (1997) 595–608.
[22] J. Fujita-Yoshigaki, Y. Dohke, M. Hara-Yokoyama, Y. Kamata, S. Kozaki, S. Furuyama, H. Sugiya, Vesicle-associated membrane protein 2 is essential for cAMP-regulated exocytosis in rat parotid acinar cells: the inhibition of cAMP-dependent amylase release by botulinum neurotoxin B, J. Biol. Chem. 271 (1996) 13130–13134.
[23] K. Simons, E. Ikonen, Functional rafts in cell membranes, Nature 387 (1997) 569–572.
[24] D.A. Brown, E. London, Functions of lipid rafts in biological membranes, Ann. Rev. Cell Dev. Biol. 14 (1998) 111–136.
[25] F. Wendler, L. Page, S. Urbe, S.A. Tooze, Homotypic fusion of immature secretory granules during maturation requires syntaxin 6, Mol. Biol. Cell 12 (2001) 1699–1709.
[26] R. Kuliawat, E. Kalinina, J. Bock, L. Fricker, T.E. McGraw, S.R. Kim, J. Zhong, R. Scheller, P. Arvan, Syntaxin-6 SNARE involvement in secretory and endocytic pathways of cultured pancreatic β-cells, Mol. Biol. Cell 15 (2004) 1690–1701.